

Quantum-mechanical and quasiclassical dynamics of coupled quasiparticle-boson systems

R. Steib

Abteilung Theoretische Physik, Universität Ulm, D-89069 Ulm, Germany

J. L. Schoendorff and H. J. Korsch

Fachbereich Physik, Universität Kaiserslautern, D-67653 Kaiserslautern, Germany

P. Reineker

Abteilung Theoretische Physik, Universität Ulm, D-89069 Ulm, Germany

(Received 10 June 1997; revised manuscript received 6 March 1998)

Statistical and dynamical properties of a quasiparticle coupled to polarization vibrations in a dimer model are investigated using a full quantum-mechanical approach. The propagation of the system is described in terms of spin-boson coherent states and compared to various quasiclassical descriptions of the system. The spectrum of the energy eigenvalues and the level spacing distributions of the system are calculated and turn out to be almost regular, especially in the strong coupling limit. It is demonstrated that the usual quasiclassical approach to this problem is not quite satisfactory. This is because the quantum fluctuations in the spin variable give rise to entangled states and correlations which hence should be included in a quasiclassical description. We show that a limited but satisfactory quasiclassical approximation may be given using a suitable integrable reference Hamiltonian. [S1063-651X(98)11406-X]

PACS number(s): 82.20.Rp, 05.45.+b, 03.65.Sq

I. INTRODUCTION

The problem of the transfer of a quasiparticle (or a particle) coupled to vibrational modes has been under strong discussion in recent years. The Davydov model [1–3] leads to a coupled set of Schrödinger equations for the occupation amplitudes of the quasiparticle. The influence of vibronic bath variables on the excitation transfer was studied in the framework of generalized Master equation [4] and stochastic Liouville equation approaches [5]. Eilbeck *et al.* [6] introduced the *discrete self-trapping equation* (DST) and studied the properties of stationary solutions. For the case of a symmetric dimer, Kenkre and Campbell [7] derived a closed nonlinear equation for the site-occupation probability difference in terms of Jacobian elliptic functions. They demonstrated the existence of a transition from a free to a self-trapped state. Later on this model was extended to include dissipation effects [8–10], asymmetry [11–15], and several other aspects [16–22]. Recently the role of nonadiabatic couplings and the role of the Born-Oppenheimer approximation in a stepwise quantization were studied [23,24].

However, it is still an open question whether such a (spin-1/2) system can be described in a quasiclassical manner at all [25,26]. Furthermore, since the quasiclassical equations show pronounced chaos for strong coupling, it is interesting to ask what happens in the quantum system itself. This has been answered partially for higher ($j \gg 1/2$) spin representations [27,28]. In Ref. [28] it was shown that in those systems the level spacing distribution tends to the universal one, expected in quantum systems where the classical dynamics shows chaos. However, for a two-level system ($j = 1/2$), the quantum dynamics is different although similar structures in classical and quantum Poincaré sections may be identified for intermediate coupling [29].

Here, we will show that a complementary approach to the

usual quasiclassical treatment of the spin-boson model may be more suitable for the spin-1/2 case. In Sec. II we present the Hamiltonian describing the system under consideration. The Hamiltonian can be split into a trivial and a nontrivial part, where the nontrivial part contains the coupling between the two subsystems (quasiparticle and vibrational degrees of freedom). The non-trivial part describes a harmonic oscillator coupled to a two-level system and is of a general type describing various physical situations in quantum optics [30–33]. Furthermore, this system represents a model for energy transfer in molecular aggregates, in doped molecular crystals and for the tunneling of particles in two-state systems [4,5]. In Sec. III A we investigate the dynamics of the system following the usual quasiclassical description. For strong coupling we find a pronounced chaotic behavior. The eigenvalues of the Hamiltonian and the level spacing distributions are presented in Sec. III B. Apparently, the eigenvalues behave quite regularly, especially in the strong coupling limit. Thus we are led to search for the integrable part of the Hamiltonian responsible for this behavior (Sec. III C), which results in approximate expressions for the eigenvalues and eigenvectors (Sec. III D). With the results of Sec. III C we are able to derive new quasiclassical equations, which are not equivalent to the previous ones. Furthermore, these equations show that the system behaves regularly in the strong coupling limit (Sec. III F). In Sec. IV we introduce quasiprobability distributions and coherent states. The dynamical behavior of the system is illustrated by means of Q functions. Various expectation values of interest are calculated and compared to the results of a pure classical description.

II. MODEL AND BASIC EQUATIONS

We consider the dynamics of a quasiparticle (or a particle, e.g., exciton or electron) in a molecular dimer. The quasipar-

particle is moving between the two sites of the dimer due to dipole-dipole interaction. The motion of the quasiparticle is coupled to local vibrational modes at the two sites. The total Hamiltonian is specified by

$$H_{\text{tot}} = H_{\text{exc}} + H_{\text{vib}} + H_{\text{int}}, \quad (1)$$

where H_{exc} , H_{vib} , and H_{int} represent the quasiparticle, the vibrational modes, and the interaction between the two subsystems, respectively:

$$H_{\text{exc}} = \varepsilon_1 A_1^\dagger A_1 + \varepsilon_2 A_2^\dagger A_2 + T(A_1^\dagger A_2 + A_2^\dagger A_1), \quad (2a)$$

$$H_{\text{vib}} = \omega_1 B_1^\dagger B_1 + \omega_2 B_2^\dagger B_2 + \frac{1}{2}(\omega_1 + \omega_2), \quad (2b)$$

$$H_{\text{int}} = g_1(B_1^\dagger + B_1)A_1^\dagger A_1 + g_2(B_2^\dagger + B_2)A_2^\dagger A_2. \quad (2c)$$

H_{exc} describes the excitation of the quasiparticle and its transfer between the two sites. A_n^\dagger, A_n ($n=1,2$) are creation and annihilation operators for the quasiparticle obeying Fermi commutation relations. ε_n is the site energy of the quasiparticle at site n and T is the transfer matrix element (dipole-dipole interaction). Throughout this paper we use $T = -0.5$ in all numerical calculations. The vibrational modes are described by H_{vib} , where ω_n are the frequencies of the intramolecular vibrations at site n . B_n^\dagger, B_n are the corresponding boson amplitude operators. The coupling between quasiparticle and vibrational degrees of freedom is specified by the interaction term H_{int} , with coupling constants g_n .

In order to simplify our Hamiltonian H_{tot} , we assume that there is exactly *one* quasiparticle excited on the dimer:

$$A_1^\dagger A_1 + A_2^\dagger A_2 = 1. \quad (3)$$

Because of Eq. (3), the quasiparticle subsystem has the properties of a spin-1/2 system. Therefore we introduce three spin operators

$$\sigma_x = A_1^\dagger A_2 + A_2^\dagger A_1, \quad (4a)$$

$$\sigma_y = -i(A_1^\dagger A_2 - A_2^\dagger A_1), \quad (4b)$$

$$\sigma_z = A_1^\dagger A_1 - A_2^\dagger A_2 \quad (4c)$$

instead of the four Fermi operators. The expectation value $\langle \sigma_z \rangle$ corresponds to the occupation difference between the two sites of the dimer. Using Eq. (3), we can show that

$$\sigma_x^2 + \sigma_y^2 + \sigma_z^2 = \text{const} \quad (5)$$

is an integral of motion and therefore the motion in σ space (subspace of the quasiparticle) is restricted to the sphere (5), the so-called Bloch sphere. It is more convenient to use polar coordinates (ϕ, θ) in the figures instead of expectation values of the spin operators. The spin operators satisfy the commutation relation (j, k, ℓ cyclic)

$$[\sigma_j, \sigma_k]_- = 2i\sigma_\ell.$$

Furthermore, new boson operators

$$B_1 = b_1 \cos \varphi - b_2 \sin \varphi, \quad (6a)$$

$$B_2 = b_1 \sin \varphi + b_2 \cos \varphi \quad (6b)$$

for the vibrational modes are introduced by a Bogoliubov transformation ($\tan \varphi = g_1/g_2$). It should be noticed that in the case of the symmetric dimer ($g_1 = g_2$), we have $\sin \varphi = \cos \varphi = 1/\sqrt{2}$ and therefore the vibrational mode b_2, b_2^\dagger corresponds to the difference of the original coordinates $q_1 - q_2$ [with $q_n = (B_n + B_n^\dagger)/\sqrt{2\omega_n}$].

Substituting Eqs. (3)–(6) and $\omega_1 = \omega_2 = \omega$ in Eq. (1) the total Hamiltonian splits into two parts:

$$H_{\text{tot}} = H_1 + H_2,$$

where H_1 represents a displaced harmonic oscillator depending only on the operators b_1 and b_1^\dagger . The nontrivial part H_2 contains the second boson mode and the coupling between the quasiparticle and second vibrational mode (b_2, b_2^\dagger). The two parts of the Hamiltonian H_1, H_2 are completely decoupled. Therefore we consider only the nontrivial part H_2 . Dropping the index ‘‘2’’ we finally obtain

$$H = -\eta \sigma_z (b^\dagger + b) + T \sigma_x + \omega \left(b^\dagger b + \frac{1}{2} \right) + \varepsilon \sigma_z + \tau (b^\dagger + b), \quad (7)$$

with the new parameters

$$\varepsilon = \frac{1}{2}(\varepsilon_2 - \varepsilon_1), \quad (8a)$$

$$\eta = \sqrt{g_1^2 + g_2^2}, \quad (8b)$$

$$\tau = \frac{1}{2} \frac{g_2^2 - g_1^2}{\sqrt{g_1^2 + g_2^2}}. \quad (8c)$$

The Heisenberg equations for this Hamiltonian read

$$\dot{\sigma}_x = -2(\varepsilon - \sqrt{2\omega\eta}Q)\sigma_y, \quad (9a)$$

$$\dot{\sigma}_y = 2(\varepsilon - \sqrt{2\omega\eta}Q)\sigma_x - 2T\sigma_z, \quad (9b)$$

$$\dot{\sigma}_z = 2T\sigma_y, \quad (9c)$$

$$\dot{Q} = P, \quad (9d)$$

$$\dot{P} = -\omega^2 Q + \sqrt{2\omega}(\eta\sigma_z - \tau). \quad (9e)$$

III. MIXED QUANTUM-CLASSICAL DYNAMICS AND SPECTRAL STATISTICS

A. First approach to a mixed quantum-classical description

A first step towards an understanding of the dynamical properties of a quantum system is the investigation of its classical counterpart. We will proceed in this direction by replacing the operators b, b^\dagger by the Hermitian position and momentum operators Q, P of the harmonic oscillator with frequency ω ,

$$Q = \frac{1}{\sqrt{2\omega}}(b^\dagger + b), \quad P = i\sqrt{\frac{\omega}{2}}(b^\dagger - b). \quad (10)$$

Rewritten in terms of these operators, the Hamiltonian (7) reads

$$H = \varepsilon \sigma_z + T \sigma_x + \sqrt{2\omega} Q (\tau - \eta \sigma_z) + \frac{1}{2} (P^2 + \omega^2 Q^2). \quad (11)$$

In this form, H can be thought of describing a spin σ_x , σ_y , σ_z coupled to an harmonic oscillator Q , P via the interaction term $\sqrt{2\omega} Q (\tau - \eta \sigma_z)$.

One way of assigning a classical interpretation to the quantum motion is to investigate the time dependence of the mean values, thus neglecting all fluctuations and correlations present in the quantum motion. In order to get the best correspondence between the classical and the quantum motion, the initial state should be an almost classical state, i.e., a state which has minimal fluctuations.

As the main assumption in our calculation, we use the initial spin-boson coherent state

$$|\psi(0)\rangle = |q_0, p_0\rangle \otimes |s_0\rangle, \quad (12)$$

where $|q, p\rangle$ represents a coherent state of the boson part and $|s\rangle$ a state of the two-level system

$$|s\rangle = |\phi, \theta\rangle = \sin(\theta/2) |\downarrow\rangle + e^{-i\phi} \cos(\theta/2) |\uparrow\rangle. \quad (13)$$

The most reasonable approximation for the time propagation is the ansatz

$$|\psi(t)\rangle = e^{i\varphi(t)} |q(t), p(t)\rangle \otimes |s(t)\rangle. \quad (14)$$

This is reasonable only if $|\psi(t)\rangle$ remains factorized and no entanglement will show up, i.e., the initial spin-boson coherent state should *not* develop as

$$|\psi(t)\rangle = c_1 |q_1, p_1\rangle \otimes |\uparrow\rangle + c_2 |q_2, p_2\rangle \otimes |\downarrow\rangle,$$

where $q_1 \neq q_2$, $p_1 \neq p_2$.

Inserting this ansatz into the *time-dependent variational principle* [34] (TDVP), and performing the variation with respect to the coordinates $q(t)$, $p(t)$, and the spin part $|s(t)\rangle$, we finally arrive at a classical set of differential equations for the behavior of the expectation values in this approximation (see Appendix A 2 for a detailed derivation):

$$\dot{s}_x = -2(\varepsilon - \sqrt{2\omega} \eta q) s_y, \quad (15a)$$

$$\dot{s}_y = 2(\varepsilon - \sqrt{2\omega} \eta q) s_x - 2T s_z, \quad (15b)$$

$$\dot{s}_z = 2T s_y, \quad (15c)$$

$$\dot{q} = p, \quad (15d)$$

$$\dot{p} = -\omega^2 q + \sqrt{2\omega} (\eta s_z - \tau). \quad (15e)$$

These equations can also be obtained by simply replacing the operators by c -numbers in the Heisenberg equations (9) according to

$$Q \mapsto q, \quad P \mapsto p, \quad \sigma_k \mapsto s_k,$$

as well as from the corresponding classical Hamiltonian [35]. This treatment of the model is often denoted as a mixed quantum-classical description. However, we want to stress that this description neglects the correlations present in the combined motion (cf. Sec. III F and Appendix A 1 for a detailed discussion).

A detailed investigation of the system (15) can be found in Ref. [35]. Here we give only a brief summary of the relevant results. The dynamics of the system in this approach is found to be both regular and chaotic. The transition from regular to chaotic behavior depends on the coupling strength η and the total energy

$$E = \varepsilon s_z + T s_x + \sqrt{2\omega} Q (\tau - \eta s_z) + \frac{1}{2} (p^2 + \omega^2 p^2) \quad (16)$$

of the system. The behavior can be analyzed by Poincaré sections in both subsystems, quasiparticle and oscillator.

We used a fourth order Runge-Kutta method [36] in connection with a method proposed by Hénon [37] allowing us to find the intersections of a trajectory with the surface of section accurately. Despite the long integration range ($\omega t \approx 10^3$), the relative errors in the two known integrals of motion, namely, the energy (16) and the radius of the Bloch sphere (5), turned out to be less than 10^{-7} . In Fig. 1 we show some typical Poincaré sections of the Bloch variables corresponding to the left turning point of the oscillator ($P = 0$, $\dot{P} > 0$).

For small values of the coupling η and low energies, the system shows regular behavior. If the energy exceeds some critical value, a stochastic layer in the vicinity of the symmetric ground state of the quasiparticle appears [Fig. 1(a)]. Increasing the energy further, chaos spreads over large parts of the Bloch sphere, leaving islands of regular behavior in the region of the energetically higher antisymmetric state of the quasiparticle. For stronger coupling, the chaotic behavior already appears at the lowest allowed energies [Fig. 1(b)]. For fixed energy, the chaotic region grows when the coupling is increased or when the oscillator frequency is decreased.

B. Spectral statistics

In the following, we restrict ourselves to the case of a symmetric dimer [$\varepsilon = \tau = 0$, cf. Eqs. (8a) and (8c)]. The Hamiltonian of the symmetric dimer,

$$H = T \sigma_x - \eta \sigma_z (b^\dagger + b) + \omega \left(b^\dagger b + \frac{1}{2} \right), \quad (17)$$

is equivalent to the Jaynes-Cummings model [30–32], which is a basic model in quantum optics. The symmetric dimer is invariant under an exchange of the two sites, i.e., the parity operator

$$\mathcal{P} = \sigma_x \exp(i\pi b^\dagger b) \quad (18)$$

commutes with H . The eigenvalues of \mathcal{P} are $p = \pm 1$ (even $\{+\}$ and odd $\{-\}$ parity).

In order to calculate the eigenvalues of the Hamiltonian (17) we expand the wave function $|\psi\rangle$ into the simultaneous eigenvectors of $b^\dagger b$ and σ_z :

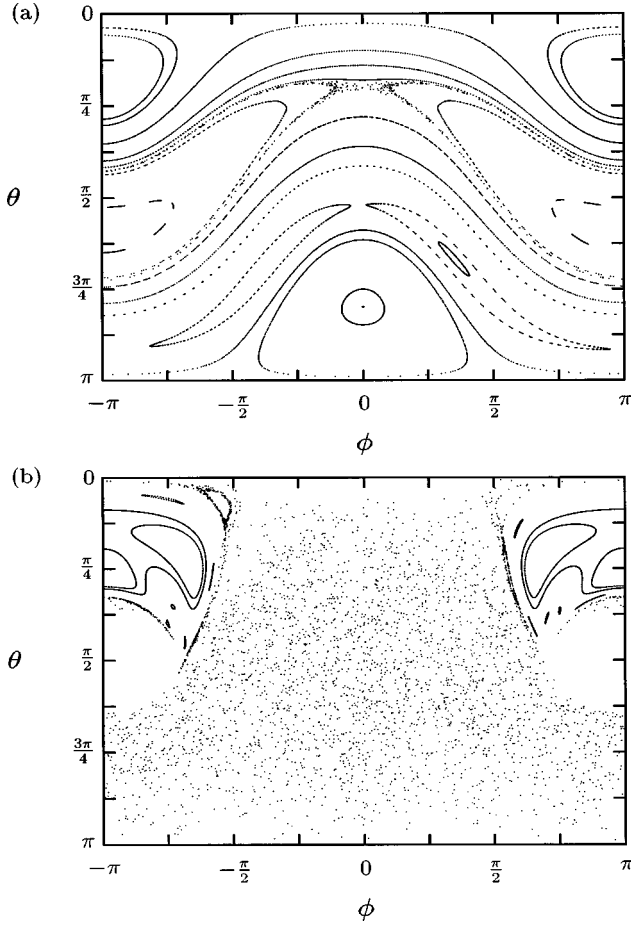


FIG. 1. Poincaré sections for weak ($\gamma=1$, $\gamma=2\eta/\omega$) and strong coupling ($\gamma=4$). In the former case (a) the formation of a stochastic layer in the vicinity of the separatrix can be seen if the energy exceeds a critical value ($E=3.0$). In the latter case (b) the whole Bloch sphere shows chaotic behavior at this energy. Chaos spreads over large parts of the Bloch sphere already for lower energies [e.g., $E=0.3$ in (b)]. In the upper part of (b) we see remaining regular elliptic islands. The region near $(\phi, \theta) = (\pm\pi, \pi/2)$ is not accessible because the energy ($E=0.3$) of the system is too low [cf. Eq. (16)].

$$|\psi\rangle = \sum_{n=0}^{\infty} C_n^{\uparrow} |n, \uparrow\rangle + \sum_{n=0}^{\infty} C_n^{\downarrow} |n, \downarrow\rangle. \quad (19)$$

In the numerical calculations we have to truncate the sums in Eq. (19) at a finite number of terms, say N . Because the eigenvalues with even and odd parity are independent, the calculation of the eigenvalues reduces to the diagonalization of two tridiagonal real $N \times N$ matrices, one for each parity $\{\pm\}$. Plotting the energy spectrum the curves with different parity $\{\pm\}$ intersect, whereas the curves with same parity show avoided level crossings (level repulsion).

For a statistical analysis of the spectrum, we calculate the spectral staircase function (the integrated level density)

$$N(E) = N\{n | E_n < E\}, \quad (20)$$

which counts the number of energy levels below the energy E . $N(E)$ can be divided into a smooth part \bar{N} and a fluctu-

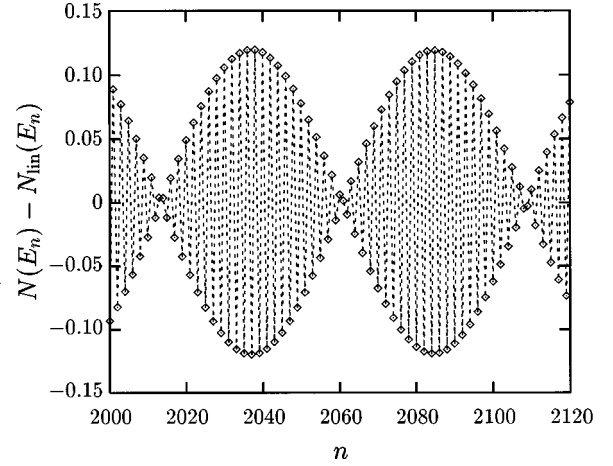


FIG. 2. Difference between the staircase function $N(E)$ and its dominant (linear) part N_{lin} as a function of n (number of the eigenvalue). As one can easily see, the deviation is oscillating regularly. This nonstatistical contribution has to be considered in the smooth part \bar{N} of the staircase function and not in the fluctuation part N_{fl} .

ating part N_{fl} . For our system the dominant behavior of the smooth part is a linear function of the energy

$$N_{\text{lin}}(E) = \frac{1}{\omega} E + \text{const.}$$

This is quite reasonable because the term $\omega b^{\dagger} b$ is the dominant part of the Hamiltonian (17), i.e., the mean level density — averaged over many (≥ 10) levels — does not depend on E . A more detailed investigation of the spectral staircase function $N(E)$ shows that the deviation

$$N(E_n) - N_{\text{lin}}(E_n)$$

from the linear behavior is oscillating quite regularly, as shown in Fig. 2. The frequency of the oscillations depends on E . When studying statistical properties of the spectrum one should take this apparently nonstatistical contribution into account in the smooth part \bar{N} . Thus we have

$$N(E) = N_{\text{lin}}(E) + N_{\text{osc}}(E) + N_{\text{fl}}(E) \quad (21a)$$

$$= \bar{N}(E) + N_{\text{fl}}(E). \quad (21b)$$

If the smooth part \bar{N} of the staircase function is known, the usual approach is to pass from the set of eigenvalues $\{E_n\}$ to the unfolded spectrum $\{E'_n\}$ using the smooth part \bar{N} of the staircase function:

$$E'_n = \bar{N}(E_n). \quad (22)$$

The unfolded spectrum $\{E'_n\}$ has a mean of unity (the quantities E'_n are dimensionless).

In order to understand this apparently regular behavior of the energy eigenvalues we consider the strong coupling limit analytically. This is done in the following section. The results of both exact numerical calculation and approximate analytical treatment are presented in Sec. III E.

C. The strong coupling limit

In this section we want to investigate the behavior of the system for strong coupling η , the range where the quasiclassical equations (15) show dominant regions of chaos in phase space. We will show that in the strong coupling limit the system is in fact nearly integrable, in the sense that we can give analytical expressions for eigenvalues and eigenvectors to this Hamiltonian to a reasonable accuracy (see also the derivations in Ref. [38]). This will be done by a suitable transformation to a new Hamiltonian (27), which extracts the integrable part of the original Hamiltonian (17). Furthermore, the quasiclassical equations (33) coming from this transformed Hamiltonian \tilde{H} show a pronounced regular behavior and the strange level spacing distribution can be reproduced analytically.

For strong coupling η , the dynamics of the system is essentially governed by the combined vibronic and two-level normal mode oscillations originating from the diagonalization of the part

$$H_{\text{vib,int}} = -\eta\sigma_z(b^\dagger + b) + \omega\left(b^\dagger b + \frac{1}{2}\right) \quad (23)$$

of the Hamiltonian H . Using the unitary transformation

$$\mathcal{U} = \exp\left(\frac{\eta}{\omega}\sigma_z(b^\dagger - b)\right) \quad (24)$$

the part $H_{\text{vib,int}}$ can be put into diagonal form. The transformation $\mathcal{U}(\eta/\omega)$ results in a replacement of the operators according to

$$\begin{aligned} b &\rightarrow \mathcal{U}^{-1}b \mathcal{U} = b + \frac{\eta}{\omega}\sigma_z, \\ b^\dagger &\rightarrow \mathcal{U}^{-1}b^\dagger \mathcal{U} = b^\dagger + \frac{\eta}{\omega}\sigma_z, \\ \sigma_x &\rightarrow \mathcal{U}^{-1}\sigma_x \mathcal{U} = \mathcal{D}\left(-\frac{2\eta}{\omega}\right)\sigma^+ + \mathcal{D}\left(\frac{2\eta}{\omega}\right)\sigma^-, \end{aligned} \quad (25)$$

where σ^\pm represent the spin flip operators

$$\sigma^+ = \begin{pmatrix} 0 & 1 \\ 0 & 0 \end{pmatrix}, \quad \sigma^- = \begin{pmatrix} 0 & 0 \\ 1 & 0 \end{pmatrix}$$

and $\mathcal{D}(\gamma)$ is the displacement operator [39]

$$\mathcal{D}(\gamma) = e^{\gamma b^\dagger - \gamma^* b}.$$

Applying the transformations to the Hamiltonian H we get the transformed one $\tilde{H} = \mathcal{U}^{-1}H\mathcal{U}$ as

$$\tilde{H} = \omega b^\dagger b + \frac{\omega}{2} - \frac{\eta^2}{\omega} + T\left[\mathcal{D}\left(-\frac{2\eta}{\omega}\right)\sigma^+ + \mathcal{D}\left(\frac{2\eta}{\omega}\right)\sigma^-\right]. \quad (26)$$

The parity operator (18) remains invariant under the transformation (24), $\mathcal{U}^{-1}\mathcal{P}\mathcal{U} = \mathcal{P}$. Instead of b, b^\dagger , we again in-

troduce the operators Q and P (10) of the harmonic oscillator and reexpress the Hamiltonian (26) in terms of these operators:

$$\tilde{H} = \frac{1}{2}(P^2 + \omega^2 Q^2) - \frac{\eta^2}{\omega} + \cos(\gamma' P)\sigma_x - \sin(\gamma' P)\sigma_y. \quad (27)$$

For simplicity of notation, we introduced the abbreviations $\gamma = 2\eta/\omega$ and $\gamma' = \gamma\sqrt{2/\omega}$. This Hamiltonian will be the starting point of a second approach to a mixed quantum-classical description (see Sec. III F).

D. Approximate calculation of the eigenvalues

As already mentioned above, the transformation \mathcal{U} diagonalizes the part $H_{\text{vib,int}}$ explicitly. The calculation presented below is a kind of perturbative treatment of the remaining part $H_{\text{exc}} = T\sigma_x$, i.e., the approximation is valid for the strong coupling–high energy case.

Calculating the eigenvalues of the transformed Hamiltonian (26), we neglect the contribution of nondiagonal boson matrix elements

$$\langle n|\tilde{H}|m\rangle, \quad n \neq m.$$

The diagonal boson matrix elements are

$$\langle n|\tilde{H}|n\rangle = \begin{pmatrix} \omega n + \frac{\omega}{2} - \frac{\eta^2}{\omega} & T\langle n|\mathcal{D}\left(\frac{2\eta}{\omega}\right)|n\rangle \\ T\langle n|\mathcal{D}\left(-\frac{2\eta}{\omega}\right)|n\rangle & \omega n + \frac{\omega}{2} - \frac{\eta^2}{\omega} \end{pmatrix}$$

and the matrix elements of $\mathcal{D}(\gamma)$ are

$$\langle n|\mathcal{D}(\gamma)|n\rangle = e^{-|\gamma|^2/2} L_n(|\gamma|^2),$$

where L_n are the Laguerre polynomials [40]. In this approximation the eigenvalues and eigenvectors for even (+) and odd (−) parity are explicitly given by

$$\tilde{E}_n^\pm = \omega n + \frac{\omega}{2} - \frac{\eta^2}{\omega} \pm (-1)^n T e^{-(2\eta^2/\omega^2)} L_n\left(\frac{4\eta^2}{\omega^2}\right). \quad (28)$$

The corresponding eigenvectors can be written as a superposition

$$|\psi_n^\pm\rangle = \frac{1}{\sqrt{2}}[|n\rangle \otimes |\uparrow\rangle \pm (-1)^n |n\rangle \otimes |\downarrow\rangle], \quad (29)$$

where $|\uparrow\rangle$ and $|\downarrow\rangle$ are eigenstates of σ_z and $|n\rangle$ are eigenstates of $b^\dagger b$. Thus the eigenvectors $|\psi_n^\pm\rangle$ have the following parity:

$$\mathcal{P}|\psi_n^\pm\rangle = \pm |\psi_n^\pm\rangle. \quad (30)$$

The results of the approximate analytical calculation of the eigenvalues (28) and the exact numerical results are presented in the following section.

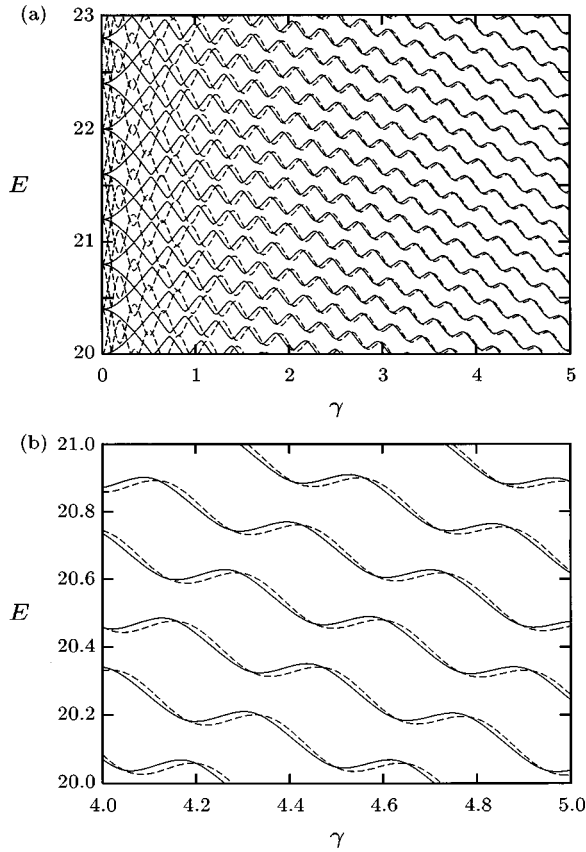


FIG. 3. Eigenvalues from an intermediate energy range (levels 100–120). The solid lines show the exact numerical calculations, whereas the dashed lines were calculated using the approximation described in the text. (a) presents an overview over a large range of the coupling ($\gamma = 2\eta/\omega$). Evidently the approximation does not hold for small couplings. For higher values of the coupling the approximation is in good agreement with the exact numerical calculations. (b) is a magnification of the lower right corner of (a). The number of Fock states is $N=800$ and the corresponding eigenfunctions have odd parity.

E. Results for the spectral statistics

In order to avoid nonuniformities at the lower end of the spectrum and truncation effects in the highest levels we used only levels from an intermediate energy range for the statistics. Furthermore it is necessary to check how many levels are reliable.

In Fig. 3 we compare the eigenvalues \tilde{E}_n [Eq. (28), strong coupling–high energy approximation] to those obtained by the exact numerical diagonalization of the Hamiltonian (17). Evidently the approximation holds for large coupling constants γ . The energy range in Fig. 3 starts with eigenvalue number 100. For higher energies the agreement is better than for smaller energies.

Because only the linear part of the staircase function is known, the spectra were unfolded using this linear part

$$E'_n = N_{\text{lin}}(E_n). \quad (31)$$

The distributions of the level spacings $s_n = E'_{n+1} - E'_n$ of the exact and the approximate calculations are compared in Fig. 4. Obviously the distributions show no significant differ-

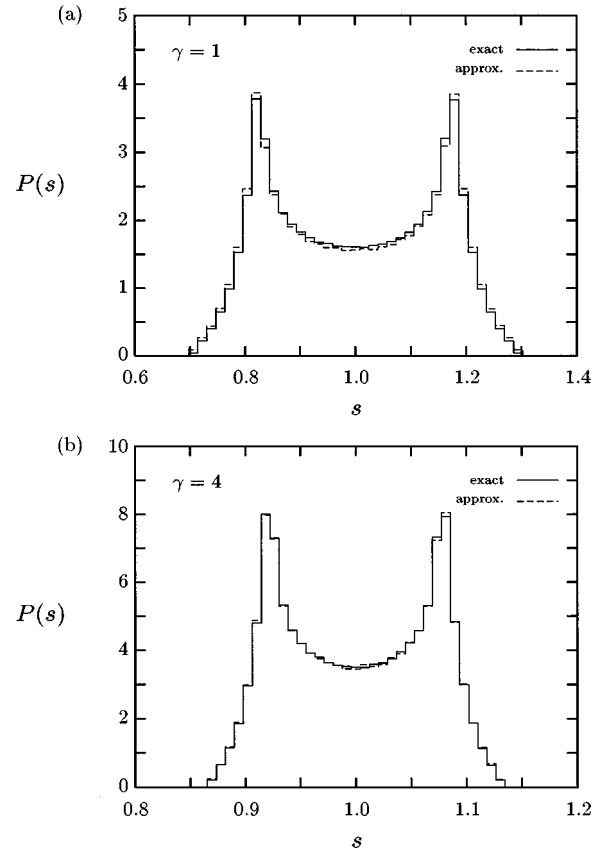


FIG. 4. Comparison of the level spacing distribution between the exact numerical calculation (solid lines) and the approximation described in the text (dashed lines). Although the approximation is valid only for large coupling strengths and high energies, the approximation leads to good results for the level statistics, even in the case of weak coupling (a). For higher coupling (b) the agreement is even better.

ences. Even for small coupling [$\gamma=1$, Fig. 4(a)], where the approximation is not too good for the levels, there are only nonsignificant differences in the distribution of the spacings. That is, the level spacing distribution can be explained using the approximate energies (28) coming from the diagonal contribution of the transformed Hamiltonian (26). In particular, the absence of small spacings, that have previously been interpreted as an evidence for quantum chaos [23,41] can be attributed to the integrable part

$$\tilde{H}_0 = \omega b^\dagger b + \frac{\omega}{2} - \frac{\eta^2}{\omega} + T e^{-2\eta^2/\omega^2} L_{b^\dagger b} \left(\frac{4\eta^2}{\omega^2} \right) \sigma_x$$

of the system [cf. Eq. (28)].

As already mentioned above, one should take the regular oscillations N_{osc} into account in the smooth part \bar{N} of the spectral staircase function. If we consider the eigenvalues coming from the approximate calculation (28) as the regular part of the spectrum, the distribution of the differences $\tilde{s}_n \equiv E_n - \tilde{E}_n$ is Poissonian, which is typical for the level spacing distributions of integrable systems.

F. Second approach to a mixed quantum-classical description

In the same way as for the Hamiltonian (7), we can derive quasiclassical equations of motion for the transformed system \tilde{H} :

$$\tilde{H} = \frac{1}{2}(P^2 + \omega^2 Q^2) - \frac{\eta^2}{\omega} + \cos(\gamma' P)\sigma_x - \sin(\gamma' P)\sigma_y.$$

Like Eq. (7) this Hamiltonian describes a harmonic oscillator coupled to a spin. However, the coupling between the spin and the oscillator is now a parametriclike coupling in which the frequency of the spin motion depends on the oscillator through higher powers of the momentum operator P . We use the same ansatz as in Sec. III A, i.e.,

$$|\tilde{\psi}(t)\rangle = |\tilde{q}(t), \tilde{p}(t)\rangle \otimes |\tilde{s}(t)\rangle,$$

where $|\tilde{q}(t), \tilde{p}(t)\rangle$ is a Bose coherent state and $|\tilde{s}(t)\rangle$ a pure quantum state of the spin subsystem. Performing the variation with respect to the coordinates $\tilde{q}(t)$, $\tilde{p}(t)$, and the spin part $|\tilde{s}(t)\rangle$, we get the following mixed set of equations (see Appendix A 3 for detailed derivations):

$$\dot{\tilde{q}} = \tilde{p} - \gamma' T e^{-(1/2)|\gamma|^2} [\sin(\gamma' \tilde{p})\tilde{s}_x + \cos(\gamma' \tilde{p})\tilde{s}_y], \quad (32a)$$

$$\dot{\tilde{p}} = -\omega^2 \tilde{q}, \quad (32b)$$

coupled to the Schrödinger equation for the spin subsystem

$$i\partial_t |\tilde{s}\rangle = T e^{-(1/2)|\gamma|^2} [\cos(\gamma' \tilde{p})\sigma_x - \sin(\gamma' \tilde{p})\sigma_y] |\tilde{s}\rangle. \quad (32c)$$

Passing to the time dependence of the mean values, we get the system

$$\dot{\tilde{s}}_x = -2T e^{-(1/2)|\gamma|^2} \sin(\gamma' \tilde{p}) \tilde{s}_z, \quad (33a)$$

$$\dot{\tilde{s}}_y = -2T e^{-(1/2)|\gamma|^2} \cos(\gamma' \tilde{p}) \tilde{s}_z, \quad (33b)$$

$$\dot{\tilde{s}}_z = 2T e^{-(1/2)|\gamma|^2} \{\sin(\gamma' \tilde{p})\tilde{s}_x + \cos(\gamma' \tilde{p})\tilde{s}_y\}, \quad (33c)$$

$$\dot{\tilde{q}} = \tilde{p} - \gamma' T e^{-(1/2)|\gamma|^2} \{\sin(\gamma' \tilde{p})\tilde{s}_x + \cos(\gamma' \tilde{p})\tilde{s}_y\}, \quad (33d)$$

$$\dot{\tilde{p}} = -\omega^2 \tilde{q}. \quad (33e)$$

If the factor $e^{-(1/2)|\gamma|^2} = e^{-2\eta^2/\omega^2}$ becomes small (intermediate and strong coupling: $\eta \approx \omega$ and $\eta \gg \omega$), the system is nearly integrable. In this case we get

$$\dot{\tilde{s}}_x \approx 0, \quad \dot{\tilde{s}}_y \approx 0, \quad \dot{\tilde{s}}_z \approx 0, \quad (34a)$$

i.e., the spin will hardly show any motion. For the oscillator we have

$$\dot{\tilde{q}} \approx \tilde{p}, \quad \dot{\tilde{p}} = -\omega^2 \tilde{q}. \quad (34b)$$

Thus oscillator and spin are almost decoupled and the system is nearly integrable.

In the small coupling case ($\eta \ll \omega$) the Hamiltonian is almost integrable as well because in this case the two subsystems are nearly decoupled. Thus in both limiting cases, the classical system of \tilde{H} shows regular behavior. Comparing the above equations (33) to the Heisenberg equations for the operators σ_k ,

$$\dot{\sigma}_x = -2T \sin(\gamma' P)\sigma_z, \quad (35a)$$

$$\dot{\sigma}_y = -2T \cos(\gamma' P)\sigma_z, \quad (35b)$$

$$\dot{\sigma}_z = 2T \{\sin(\gamma' P)\sigma_x + \cos(\gamma' P)\sigma_y\}, \quad (35c)$$

and the operators Q and P ,

$$\dot{Q} = P - \gamma' T \{\sin(\gamma' P)\sigma_x + \cos(\gamma' P)\sigma_y\}, \quad (35d)$$

$$\dot{P} = -\omega^2 Q, \quad (35e)$$

we recognize the same structure. The transfer matrix element T , however, is effectively reduced to

$$T \rightarrow T \exp(-|\gamma|^2/2),$$

which is caused by the fluctuations

$$\langle P^n \rangle - \langle P \rangle^n \neq 0$$

in the boson mode.

IV. QUANTUM-MECHANICAL DYNAMICS

A. Time evolution and initial states

In this section we investigate the time evolution of the state vector $|\psi(t)\rangle$ for various initial conditions. The time propagation has been calculated in the basis of the simultaneous eigenvectors of $b^\dagger b$ and σ_z as in Eq. (19):

$$|\psi(t)\rangle = \sum_{n=0}^{\infty} C_n^\uparrow(t) |n, \uparrow\rangle + \sum_{n=0}^{\infty} C_n^\downarrow(t) |n, \downarrow\rangle. \quad (36)$$

In this representation the Schrödinger equation

$$i\partial_t |\psi(t)\rangle = H |\psi(t)\rangle$$

for the Hamiltonian (7) is equivalent to the set of first order differential equations for the coefficients $C_n^\uparrow(t)$ and $C_n^\downarrow(t)$:

$$i\partial_t C_n^\uparrow(t) = \sum_m H_{n,m}^{\uparrow\uparrow} C_m^\uparrow(t) + \sum_m H_{n,m}^{\uparrow\downarrow} C_m^\downarrow(t),$$

$$i\partial_t C_n^\downarrow(t) = \sum_m H_{n,m}^{\downarrow\uparrow} C_m^\uparrow(t) + \sum_m H_{n,m}^{\downarrow\downarrow} C_m^\downarrow(t),$$

with the matrix elements

$$H_{n,m}^{\uparrow\uparrow} \equiv \langle n, \uparrow | H | m, \uparrow \rangle = (n+1/2)\omega \delta_{n,m} - \eta(\sqrt{n} \delta_{n,m+1} + \sqrt{n+1} \delta_{n,m-1}),$$

$$H_{n,m}^{\downarrow\downarrow} \equiv \langle n, \downarrow | H | m, \downarrow \rangle = (n+1/2)\omega \delta_{n,m} + \eta(\sqrt{n} \delta_{n,m+1} + \sin(\theta_0/2) |q_0 + \gamma'/2, p_0\rangle \otimes |\downarrow\rangle), \quad (39)$$

$$+ \sqrt{n+1} \delta_{n,m-1}),$$

$$H_{n,m}^{\uparrow\downarrow} \equiv \langle n, \uparrow | H | m, \downarrow \rangle = T \delta_{n,m},$$

$$H_{n,m}^{\downarrow\uparrow} \equiv \langle n, \downarrow | H | m, \uparrow \rangle = T \delta_{n,m}.$$

The time evolution has been calculated for certain initial spin-boson coherent states

$$|\psi(0)\rangle = |q_0, p_0\rangle \otimes |s_0\rangle, \quad s_0 = (\phi_0, \theta_0) \quad (37)$$

i.e., coherent states for both subsystems. The coefficients are given by

$$C_n^{\uparrow}(0) = e^{-(1/2)|\beta_0|^2} \frac{\beta_0^n}{\sqrt{n!}} e^{-i\phi_0} \cos(\theta_0/2),$$

$$C_n^{\downarrow}(0) = e^{-(1/2)|\beta_0|^2} \frac{\beta_0^n}{\sqrt{n!}} \sin(\theta_0/2),$$

with

$$\beta = \sqrt{\frac{\omega}{2}} q + \frac{i}{\sqrt{2\omega}} p, \quad \beta^* = \sqrt{\frac{\omega}{2}} q - \frac{i}{\sqrt{2\omega}} p.$$

In order to get a valuable image of the inherent correlations and fluctuations of the quantum motion, we illustrate the dynamical behavior by means of the four Q functions Q_j , $j=0, \dots, 3$

$$Q_j(\beta, t) = \text{Tr}\{\sigma_j |\beta\rangle \langle \beta | \rho(t)\}. \quad (38)$$

The representation in terms of Q functions proves to be most suitable, because they are built upon coherent states and thus reflect most of the classical dynamics hidden in the quantum motion [39,42–45].

B. Time propagation in the transformed system

The time dependence of a state vector $|\psi(t)\rangle$ governed by the original Hamiltonian H (7) may equivalently be described by a state vector $|\tilde{\psi}(t)\rangle$ governed by the Hamiltonian \tilde{H} (26):

$$|\tilde{\psi}(t)\rangle = \exp(-i\tilde{H}t) |\tilde{\psi}(0)\rangle.$$

The relation between corresponding states

$$|\tilde{\psi}(t)\rangle = \mathcal{U}^{-1} |\psi(t)\rangle = \exp\left(-\frac{\eta}{\omega} \sigma_z (b^\dagger - b)\right) |\psi(t)\rangle$$

and operators $\tilde{X} = \mathcal{U} X \mathcal{U}^{-1}$ is given via the unitary transformation $\mathcal{U}(\eta/\omega)$. For an initially coherent state

$$|\psi_0\rangle = |q_0, p_0\rangle \otimes |s_0\rangle = |q_0, p_0\rangle \otimes |(\phi_0, \theta_0)\rangle$$

we get

$$|\tilde{\psi}_0\rangle = e^{-i\phi_0} [\cos(\theta_0/2) |q_0 - \gamma'/2, p_0\rangle \otimes |\uparrow\rangle$$

where $\gamma' = (2\eta/\omega)\sqrt{2/\omega}$ as before.

Considering the dynamics of the transformed system (27), it is found from the classical equations (33) that — in the strong coupling limit — the spin part shows only a minor time dependence, whereas the boson mode performs a simple rotation in its phase space, the (q, p) plane.

C. Trapped states

Starting with a spin-boson coherent state polarized in positive σ_z direction,

$$|\psi_0\rangle = |q_0, p_0\rangle \otimes |\uparrow\rangle, \quad (40)$$

one has to consider the time dependence of the state $|\tilde{\psi}_0\rangle$ where

$$|\tilde{\psi}_0\rangle = |q_0 - \gamma'/2, p_0\rangle \otimes |\uparrow\rangle. \quad (41)$$

This is obviously a spin-boson coherent state with $\tilde{q}_0 = q_0 - \gamma'/2$, $\tilde{p}_0 = p_0$. In the transformed system the classical motion shows only a simple time dependence [cf. Eq. (34)]. The spin remains almost constant,

$$\tilde{s}_i \approx \text{const},$$

whereas the boson part performs a simple rotation in the oscillator phase space:

$$\tilde{q}(t) = \tilde{q}_0 \cos(\omega t) + (\tilde{p}_0/\omega) \sin(\omega t),$$

$$\tilde{p}(t) = \tilde{p}_0 \cos(\omega t) - \omega \tilde{q}_0 \sin(\omega t).$$

The time dependence of $|\tilde{\psi}(t)\rangle$ can now be approximated by the expression

$$|\tilde{\psi}(t)\rangle = e^{i\varphi(t)} |\tilde{q}_0, \tilde{p}_0\rangle \otimes |\uparrow\rangle.$$

The additional phase $\varphi(t)$ accounts for the time dependence of the quantum phase, see Appendix A. In the original system (applying the transformation \mathcal{U} to the corresponding operators) $q(t)$ and $p(t)$ are explicitly given by

$$q(t) = \gamma'/2 + (q_0 - \gamma'/2) \cos(\omega t) + (p_0/\omega) \sin(\omega t),$$

$$p(t) = p_0 \cos(\omega t) - \omega(q_0 - \gamma'/2) \sin(\omega t).$$

Hence $|\psi(t)\rangle$ will perform an elliptic motion around the center $q = \gamma'/2$, $p = 0$ where the two major axes are given by $\Delta q = q_0 - \gamma'/2$ and $\Delta p = p_0$. In particular, for the initial state $q_0 = \gamma'/2$ and $p_0 = 0$, the state vector will show no motion and thus will appear to be trapped at this point. Obviously the same arguments will hold for a state polarized in negative σ_z direction:

$$|\psi_0\rangle = |q_0, p_0\rangle \otimes |\downarrow\rangle.$$

In this case, $|\psi(t)\rangle$ will perform an elliptic motion around the center $q = -\gamma'/2$, $p = 0$ with the two major axes given by $\Delta q = q_0 + \gamma'/2$ and $\Delta p = p_0$. For the initial state $q_0 =$

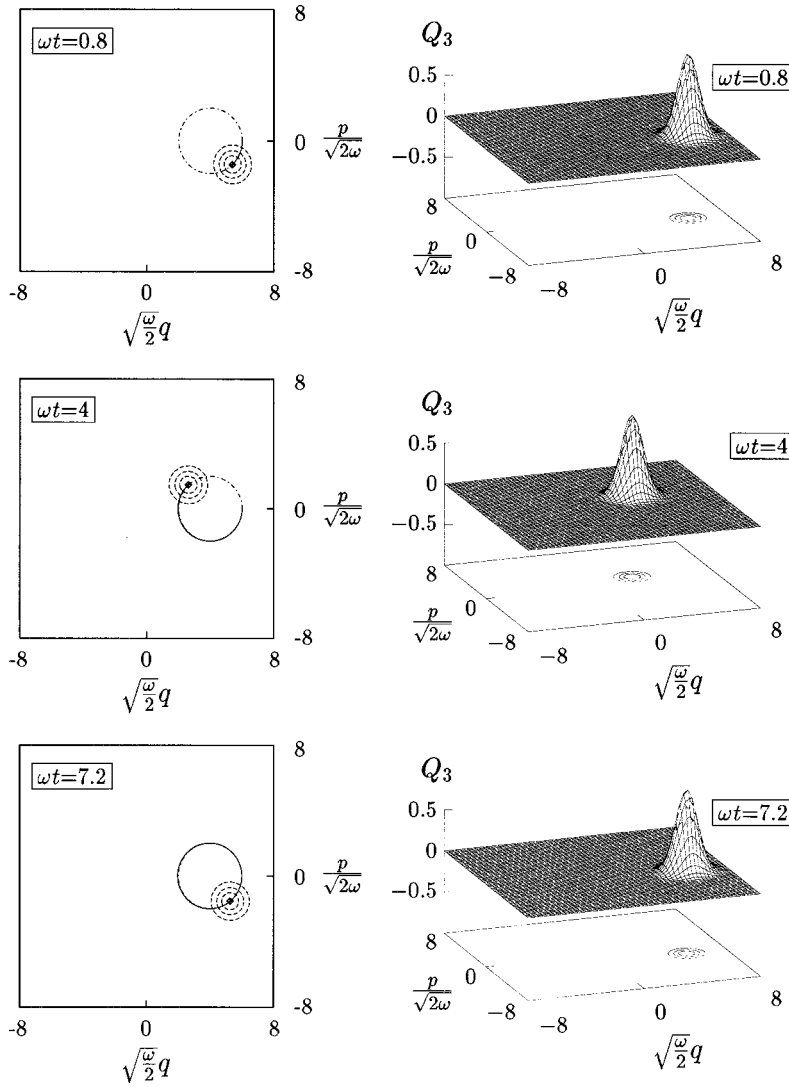


FIG. 5. Time evolution of quantum vs quasi-classical description in the oscillator phase space for the initial state $|q_0 = \frac{3}{2}q_{\text{tr}}^+, p_0 = p_{\text{tr}}^+\rangle \otimes |\uparrow\rangle$ ($\gamma = 4$). In the left-hand side of the figure, the solid line represents the quantum trajectory up to the indicated time ($\omega t = 0.8, 4, 7.2$). The final point of the trajectory is marked by a square. For the quasi-classical description we used a dashed line for the trajectory and a cross for the final point. Additionally the contour lines of the Q function $Q_3(t)$ are plotted. The right-hand side shows the Q function $Q_3(t)$, where the spin orientation can be seen. For detailed explanations see the text.

$-\gamma'/2$ and $p_0 = 0$ the state vector will appear to be trapped as well. Thus the state vectors

$$|\psi_{\text{tr}}^+\rangle = |q_{\text{tr}}^+ = \gamma'/2, p_{\text{tr}}^+ = 0\rangle \otimes |\uparrow\rangle,$$

$$|\psi_{\text{tr}}^-\rangle = |q_{\text{tr}}^- = -\gamma'/2, p_{\text{tr}}^- = 0\rangle \otimes |\downarrow\rangle$$

will remain almost constant in time. This fits perfectly to the exact quantum treatment calculated numerically using the expansion (36) for the state vector. The infinite sums were truncated at an appropriate number of states N . This number is determined by the dynamical behavior of the system. One has to make sure that the contribution of the states with $n > N$ is negligible by checking the distributions of $|C_n^+(t)|^2$ and $|C_n^-(t)|^2$ which must decrease sufficiently fast for $n \rightarrow N$.

D. States starting in the “vicinity” of a trapped state

For states starting in the “vicinity” of a trapped state we expect that the spin state remains nearly constant, whereas the oscillator will perform a rotation in the phase space around the center $(q_{\text{tr}}^+, p_{\text{tr}}^+)$, the location of the trapped state.

In Fig. 5 such a state

$$|\psi_0\rangle = \left| q_0 = \frac{3}{2}q_{\text{tr}}^+, p_0 = p_{\text{tr}}^+ \right\rangle \otimes |\uparrow\rangle,$$

starting in the “vicinity” of the trapped one is plotted. The Q function performs the expected rotation in the phase space of the oscillator. The circle corresponding to the rotation is plotted as a dash-dotted line in the figure. At least the oscillator variables can be described by the classical treatment [see Fig. 6(a)].

The spin variables show very small oscillations but the behavior of the mean value of the spin operator varies smoothly as compared to the fast oscillations of its quasiclassical counterparts [Figs. 6(b) and 6(c)].

E. Switching the spin orientation

The next initial state we want to discuss is

$$|q_0 = q_{\text{tr}}^+, p_0 = p_{\text{tr}}^+\rangle \otimes |\downarrow\rangle,$$

i.e., the boson part fits to the trapped state $|\psi_{\text{tr}}^+\rangle$, but the state of the spin system is switched from $|\uparrow\rangle$ to $|\downarrow\rangle$. For this state we can — as a simple approximation — assume that it behaves like a state starting near the trapped state $|\psi_{\text{tr}}^-\rangle$ and

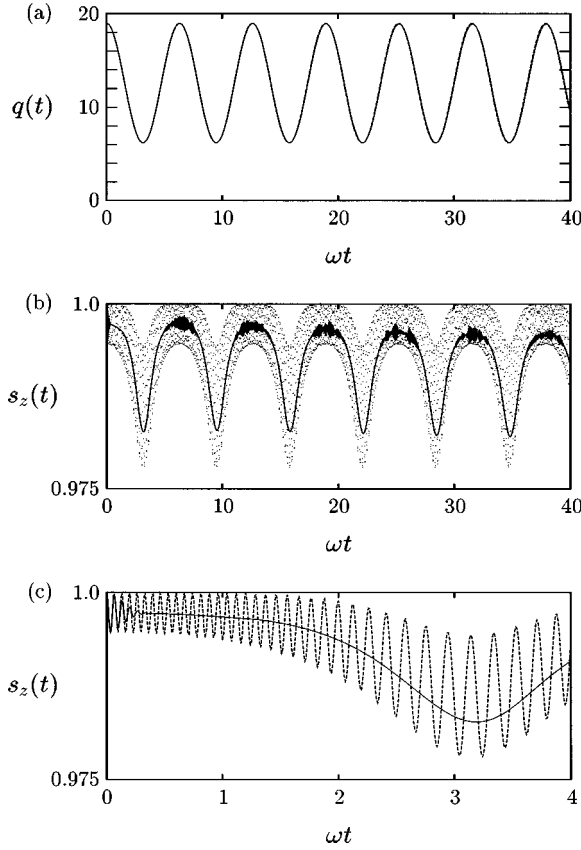


FIG. 6. Quantum expectation values (solid lines) vs quasiclassical description [dashed lines, respectively dotted lines in (b)] for the oscillator coordinate $q(t)$ and the occupation difference $s_z(t)$ for the same initial state as in Fig. 5. There is no significant difference between quantum and quasiclassical calculation concerning the oscillator variables, whereas the quantum mean value $s_z(t)$ of the spin operator varies smoothly as compared to its quasiclassical counterpart.

thus performs a rotation around the center $(q_{\text{tr}}^-, p_{\text{tr}}^-)$. But we have to stress that it is starting at a considerable distance from the point $(q_{\text{tr}}^-, p_{\text{tr}}^-)$.

In Fig. 7 we have plotted the time evolution of the Q function Q_3 for this state. We recognize the largest peak rotating around the center $(q_{\text{tr}}^-, p_{\text{tr}}^-)$ (dash-dotted circle). The negative values of Q_3 show that this rotating peak is correlated with the spin state $|\downarrow\rangle$.

The additional small structures, which become more and more enhanced as time goes on, can be addressed to small, but still existing correlations. Regarding the time evolution of this state it is obvious that the state splits into three coherently superposed packets, which are themselves correlated with different spin states.

We also perceive that up to $\omega t = 4$ the quasiclassical and quantum trajectories lie close together. Later in time they drift more and more away from each other. This is due to the contribution of the additional structures. The classical trajectory apparently follows the peak moving outside the dash-dotted circle.

F. Superposition of states

Now we consider as an initial condition a spin-boson coherent state polarized in the positive σ_x direction:

$$|\psi_0\rangle = |q_0, p_0\rangle \otimes (|\uparrow\rangle + |\downarrow\rangle) / \sqrt{2}.$$

The transformed state can be expressed as a superposition of two states

$$|\tilde{\psi}\rangle = (|\tilde{\psi}_0^+\rangle + |\tilde{\psi}_0^-\rangle) / \sqrt{2},$$

where the two parts are given by

$$|\tilde{\psi}_0^+\rangle = |q_0 - \gamma'/2, p_0\rangle \otimes |\uparrow\rangle,$$

$$|\tilde{\psi}_0^-\rangle = |q_0 + \gamma'/2, p_0\rangle \otimes |\downarrow\rangle.$$

Obviously $|\tilde{\psi}_0\rangle$ does not represent a simple product state as in Sec. IV C, however, it may be interpreted as the superposition of the two orthogonal spin-boson coherent states $|\tilde{\psi}_0^+\rangle$ and $|\tilde{\psi}_0^-\rangle$ which are nearly dynamically independent.

In Fig. 8, we have illustrated the time evolution of such a state, namely,

$$|\psi\rangle = |q_0 = q_{\text{tr}}^+, p_0 = p_{\text{tr}}^+\rangle \otimes \frac{1}{\sqrt{2}} (|\uparrow\rangle + |\downarrow\rangle).$$

The quantum motion is thus the superposition coming from the nearly independent motion of the two spin-boson coherent states as discussed in the previous sections. At first we have the trapped state $|\psi_0^+\rangle$ (see Sec. IV C) which is almost motionless. On the other hand, we have the state discussed in Sec. IV E.

In Fig. 8 both parts can be identified clearly. The values of Q_3 show that the moving peak is correlated with the spin state $|\downarrow\rangle$ whereas the trapped peak is correlated with the spin state $|\uparrow\rangle$.

Thus we have strong correlations realized by the two peaks moving in the phase space of the oscillator where (in contrast to the initial state) each peak is now correlated with a different spin orientation. The time evolution of the corresponding state shows an extremely nonclassical behavior, which can *not* be described by a product ansatz

$$|\psi(t)\rangle \neq |q(t), p(t)\rangle \otimes |s(t)\rangle.$$

Here the quasiclassical and quantum trajectories drift away from each other very early. A quasiclassical description is not possible for such a state.

However, since the overlap between both ‘‘partial states’’ is negligible, it is possible to interpret the respective time evolution with the help of two coherently superposed states, if one includes the additional phase coming from the TDVP (see Appendix A 1).

G. Time evolution of the occupation difference

In Fig. 9 the quantum mean values s_z for the different initial states described above are plotted:

$$(a) \quad |\psi_0\rangle = |q_0 = q_{\text{tr}}^+, p_0 = p_{\text{tr}}^+\rangle \otimes |\uparrow\rangle = |\psi_{\text{tr}}^+\rangle,$$

$$(b) \quad |\psi_0\rangle = |q_0 = q_{\text{tr}}^+, p_0 = p_{\text{tr}}^+\rangle \otimes |\downarrow\rangle,$$

$$(c) \quad |\psi_0\rangle = |q_0 = q_{\text{tr}}^+, p_0 = p_{\text{tr}}^+\rangle \otimes (|\uparrow\rangle + |\downarrow\rangle) / \sqrt{2}.$$

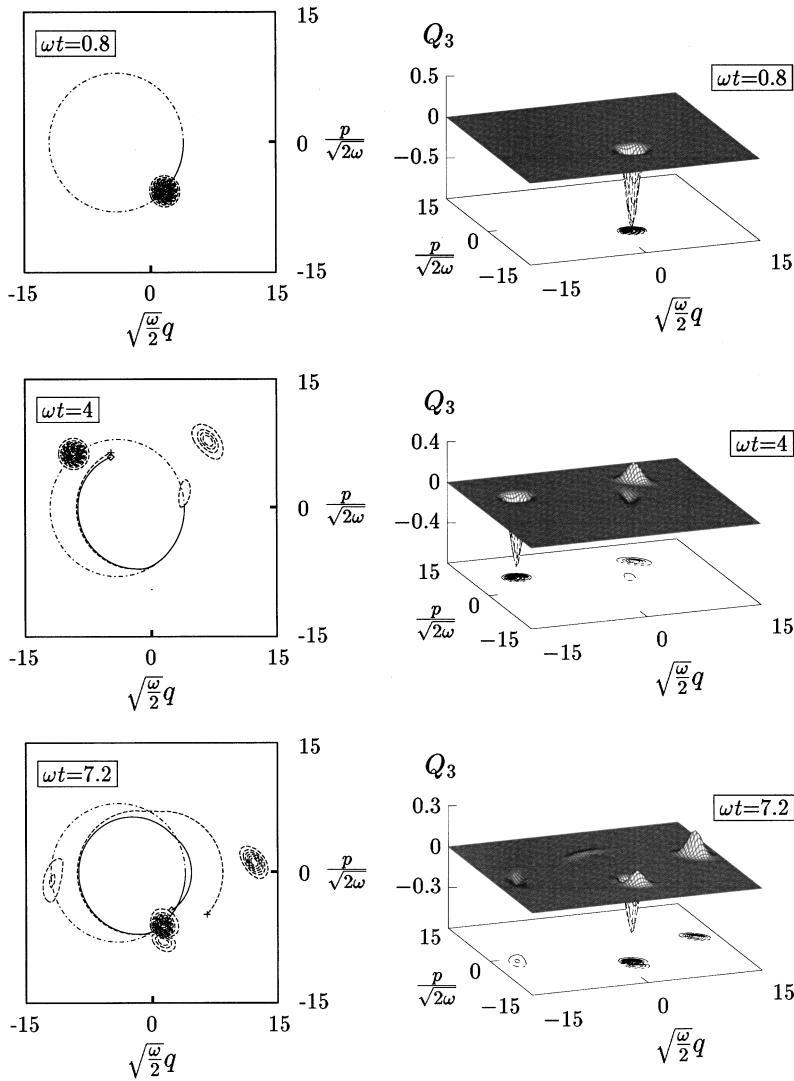


FIG. 7. The same as Fig. 5 for a different initial state: $|q_0 = q_{tr}^+, p_0 = p_{tr}^+ \rangle \otimes |\downarrow\rangle$.

First, in Fig. 9(a) we have the trapped state where the spin is nearly constant as it is expected from the quasiclassical description.

The strange time dependence of s_z in Figs. 9(b) and 9(c) cannot be described by the simple product ansatz (14), but may be captured by an improved description including entangled states in the quasiclassical treatment using the TDVP.

V. CONCLUSIONS

We have investigated the properties of a system described by a harmonic oscillator coupled to a two-level system. This model describes various interesting physical situations, e.g., a quasiparticle coupled to polarization vibrations in a dimer model. Such dimers may be realized as molecular dimers or as dimer traps in, e.g., an organic solid. Dimers are also frequently used model systems for the investigation of the electronic energy transport in solids. Thus a more thorough understanding of the energy transport in dimers also contributes to a better understanding of the energy transport in solid.

We used an approach complementary to the usual quasiclassical treatment. Identifying an integrable Hamiltonian in the strong coupling case, we found that, especially in the strong coupling limit, the system is nearly integrable in con-

trast to the pronounced chaotic behavior of the usual quasiclassical description. Although both Hamiltonians considered are equivalent (related by a unitary transformation \mathcal{U}), the resulting quasiclassical equations are not.

Furthermore, the two sets of quasiclassical equations lead to a qualitatively different behavior. The reason for these discrepancies is that the unitary transformation \mathcal{U} will turn a product state into an entangled state and vice versa. Thus the transition from the quantum description to the quasiclassical approximation depends on the selection of a suitable reference Hamiltonian.

If the entire time evolution given by the Schrödinger equation of an initial product state of coherent states can be expressed as a product state

$$|q(t), p(t)\rangle \otimes |s(t)\rangle = \exp(-i\tilde{H}t) |q(0), p(0)\rangle \otimes |s(0)\rangle$$

in the course of time, the corresponding quasiclassical equations derived from \tilde{H} are expected to give reasonable results. Therefore the quasiclassical description can only be adequate for certain initial conditions of the system. In a spin-1/2 system, however, the quantum fluctuations in the spin variables

$$\sqrt{\langle \sigma^2 \rangle - \langle \sigma \rangle^2}$$

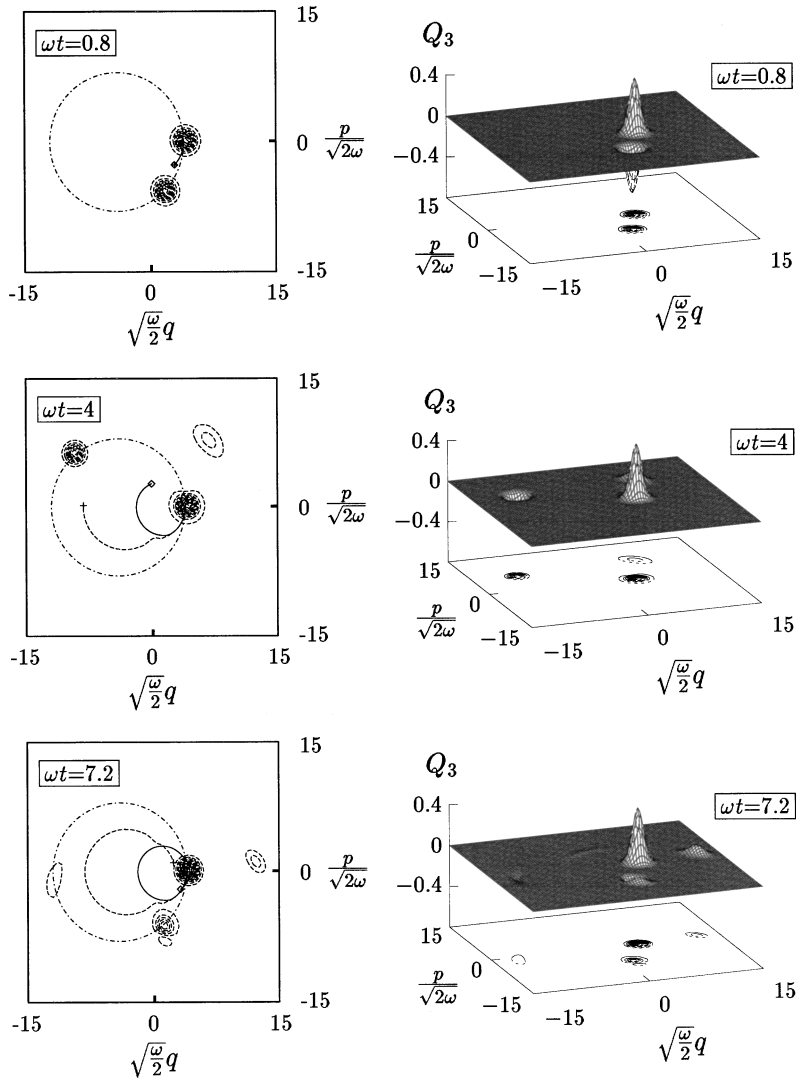


FIG. 8. The same as in Fig. 5 for a different initial state: $|q_0 = q_{tr}^+, p_0 = p_{tr}^+ \rangle \otimes 1/\sqrt{2} (|\uparrow\rangle + |\downarrow\rangle)$.

are very large (of order $\langle \sigma \rangle$). This leads to highly entangled states which are very common in this model. Thus a reasonable description of such systems with inherent large quantum fluctuations and thus extremely nonclassical states should be described by tools, which include both fluctuations and entanglement of the two subsystems, in a straightforward manner. This will lead to more degrees of freedom in the TDVP.

The main purpose of the paper was the investigation of the connection between the full quantum-mechanical solution and various classical approximations in the strong coupling case. An experimental test of the results should be possible on systems mentioned in the Introduction and above using short-time, pump-probe, coherent, or Raman spectroscopy.

ACKNOWLEDGMENTS

We appreciate valuable discussions with A. Engelmann. Financial support from the Deutsche Forschungsgemeinschaft (DFG) is gratefully acknowledged. One of the authors (P.R.) acknowledges discussions with H. Morawitz and a NATO Collaborative Research Grant.

APPENDIX A: QUASICLASSICAL EQUATIONS

1. The time-dependent variational principle

There are various qualitatively different ways to construct mixed equations of motion where one component of the system is treated classically and the other purely quantum mechanically. The most reasonable approach is to write down the equation of motion for the classical part and the Schrödinger equation for the quantum part. The coupling between these two components is approximated by a coupling taking into account only the expectation values of the quantum system. This may be considered as a self-consistent or mean-field approximation to the combined dynamics. However, one should keep in mind that following this procedure certainly neglects the fluctuations present in the nearly classical system. Even more restrictive, also certain correlations which will show up as time goes on are not included here.

In order to deal with these aspects in a uniform way we use the *time-dependent variational principle* [34] to construct self-consistent equations of motion for mixed quantum-classical systems. This formalism takes the quantum fluctuations, present in the nearly classical system, into account in a straightforward manner. Further this method is — depending on the ansatz — capable of accounting for

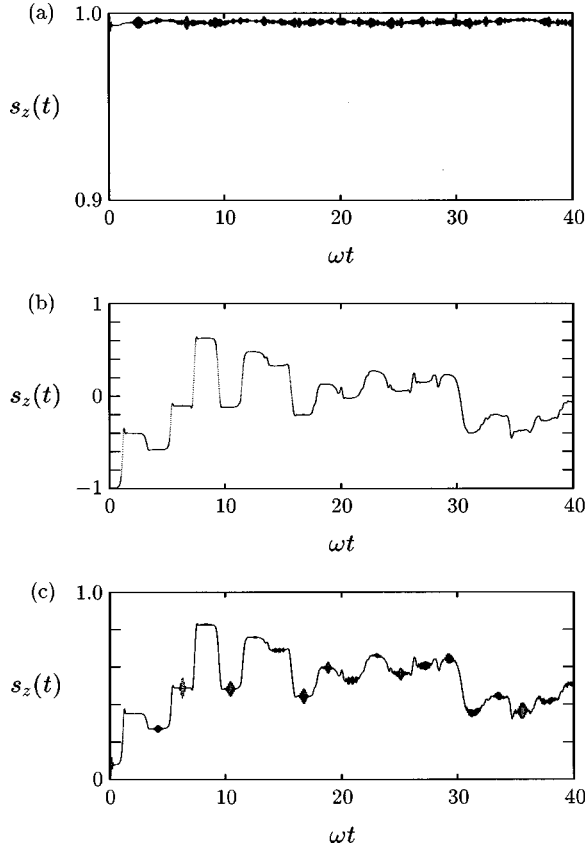


FIG. 9. Time evolution of the occupation difference $s_z(t)$ (quantum-mechanical treatment) for the strong coupling case ($\gamma = 4$). The initial state corresponding to (a) is the trapped state $|\psi_{tr}^+\rangle$, whereas the initial states for (b) and (c) are the same as in Fig. 7, respectively, Fig. 8.

entangled states, which might occur in the course of time.

The TDVP is based on the simple fact that the stationary points $\psi_c(t)$ of the action functional

$$S[\psi] = \int dt \langle \psi(t) | \{-i\partial_t + H\} | \psi(t) \rangle = \int dt \mathcal{L} \quad (\text{A1})$$

($\langle \psi | \psi \rangle = 1$) are just the solutions of the Schrödinger equation [46]. As a brief example let us consider a harmonic oscillator, the subsystem 1, coupled to a second (quantum) system. The Hamiltonian of the combined system reads

$$H = \frac{1}{2}(P^2 + \omega^2 Q^2) + H_2 + F_1(Q, P)F_2, \quad (\text{A2})$$

where F_1 depends only on the operators Q, P of subsystem 1, H_2 is the Hamiltonian of the subsystem 2, and F_2 depends only on operators of subsystem 2.

Assuming that the combined quantum system behaves nearly classically, i.e., the correlation between boson (q, p) and spin (ϕ) degrees of freedom are negligible, we are led to the factorized ansatz

$$|\psi(t)\rangle = e^{i\varphi(t)} |q(t), p(t)\rangle \otimes |\phi(t)\rangle, \quad (\text{A3})$$

where $|q(t), p(t)\rangle$ is a coherent state of the oscillator and $|\phi(t)\rangle$ is a state of the second subsystem alone. The reason

for inserting the phase $\varphi(t)$ will become clear later. If we plug this test function into the TDVP, we get the Lagrangian \mathcal{L} ,

$$\begin{aligned} \mathcal{L} = & \dot{\varphi} + \frac{1}{2}(q\dot{p} - p\dot{q}) + \frac{1}{2}(p^2 + \omega^2 q^2) + \frac{\omega}{2} \\ & + \langle \phi | \{-i\partial_t + H_2\} | \phi \rangle + \langle q, p | F_1(Q, P) | q, p \rangle \langle \phi | F_2 | \phi \rangle. \end{aligned}$$

The variation of this Lagrangian with respect to $q(t)$, $p(t)$, and $\phi(t)$ leads to the equations of motion

$$\dot{q} = p, \quad (\text{A4a})$$

$$\dot{p} = -\omega^2 q - \partial_q \bar{F}_1(q, p) \langle \phi | F_2 | \phi \rangle, \quad (\text{A4b})$$

$$i\partial_t | \phi \rangle = \{H_2 + \bar{F}_1(q, p) F_2\} | \phi \rangle, \quad (\text{A4c})$$

with $\bar{F}_1(q, p) = \langle q, p | F_1(Q, P) | q, p \rangle$. Both symbols \bar{F}_1 and F_1 do not coincide in general, unless $F_1(Q, P)$ is a linear function of Q and P .

However, since the phase $\varphi(t)$ enters into the Lagrangian \mathcal{L} only via a total time derivative, φ itself will not appear in the equations of motion. Due to this gauge invariance of the equation of motion with respect to the phase φ , it has to be fixed in addition according to

$$\int dt \langle \psi(t) | \{-i\partial_t + H\} | \psi(t) \rangle = 0. \quad (\text{A5})$$

Therefore the phase φ may be omitted in the construction of the quasiclassical equations of motion for this combined subsystem.

2. Equations from the Hamiltonian H

To derive the quasiclassical equations from the Hamiltonian H of the first approach (11) we use the TDVP ansatz

$$|\psi(t)\rangle = |q(t), p(t)\rangle \otimes |s(t)\rangle. \quad (\text{A6})$$

Inserting this into the Lagrangian \mathcal{L} and performing the variation with respect to the coordinates $q(t)$, $p(t)$, and the spin part $|s(t)\rangle$ we finally arrive at a coupled set of differential equations for the approximate behavior of the mean values ($s_k = \langle s | \sigma_k | s \rangle$):

$$\dot{s}_x = -2(\varepsilon - \sqrt{2\omega}\eta q)s_y, \quad (\text{A7a})$$

$$\dot{s}_y = 2(\varepsilon - \sqrt{2\omega}\eta q)s_x - 2Ts_z, \quad (\text{A7b})$$

$$\dot{s}_z = 2Ts_y, \quad (\text{A7c})$$

and the oscillator variables

$$\dot{q} = p, \quad (\text{A7d})$$

$$\dot{p} = -\omega^2 q + \sqrt{2\omega}(\eta s_z - \tau). \quad (\text{A7e})$$

It is worthwhile to note that these equations take the same form as if one calculates the Heisenberg equations and then passes to a classical description by considering all operators

as c -numbers. Both prescriptions coincide here but only because the various operators of the subsystems occur only in linear combinations.

3. Equations from Hamiltonian \tilde{H}

To derive the quasiclassical equations for the Hamiltonian of the second approach (27), we use the same formalism as in the preceding section and we get the following set of differential equations ($\tilde{s}_k = \langle \tilde{s} | \sigma_k | \tilde{s} \rangle$):

$$\dot{\tilde{s}}_x = -2Te^{-(1/2)|\gamma|^2} \sin(\gamma' \tilde{p}) \tilde{s}_z,$$

$$\dot{\tilde{s}}_y = -2Te^{-(1/2)|\gamma|^2} \cos(\gamma' \tilde{p}) \tilde{s}_z,$$

$$\dot{\tilde{s}}_z = 2Te^{-(1/2)|\gamma|^2} \{\sin(\gamma' \tilde{p}) \tilde{s}_x + \cos(\gamma' \tilde{p}) \tilde{s}_y\},$$

$$\dot{\tilde{q}} = \tilde{p} - \gamma' Te^{-(1/2)|\gamma|^2} \{\sin(\gamma' \tilde{p}) \tilde{s}_x + \cos(\gamma' \tilde{p}) \tilde{s}_y\},$$

$$\dot{\tilde{p}} = -\omega^2 \tilde{q}.$$

Unlike in the preceding section, these equations are not linear in Q and P , which effectively leads to the modification of the transfer matrix element T discussed in Sec. III F.

-
- [1] A. S. Davydov, *Theory of Molecular Excitations* (Plenum Press, New York, 1971).
- [2] A. S. Davydov and N. I. Kislukha, *Phys. Status Solidi B* **59**, 465 (1973).
- [3] A. S. Davydov, *J. Theor. Biol.* **38**, 559 (1973).
- [4] V. M. Kenkre, in *Exciton Dynamics in Molecular Crystals and Aggregates*, edited by G. Höhler (Springer-Verlag, Berlin, 1982).
- [5] P. Reineker, in *Exciton Dynamics in Molecular Crystals and Aggregates*, edited by G. Höhler (Springer-Verlag, Berlin, 1982).
- [6] J. K. Eilbeck, P. S. Lomdahl, and A. C. Scott, *Physica D* **16**, 318 (1985).
- [7] V. M. Kenkre and D. K. Campbell, *Phys. Rev. B* **34**, 4959 (1986).
- [8] V. Szöcs and P. Baňacký, *Phys. Rev. A* **45**, 5415 (1992).
- [9] V. Szöcs, P. Baňacký, and A. Zajac, *Phys. Rev. A* **45**, 737 (1990).
- [10] V. Szöcs, P. Baňacký, and P. Reineker, *Chem. Phys.* **199**, 1 (1995).
- [11] B. Esser and D. Hennig, *Z. Phys. B* **83**, 285 (1991).
- [12] B. Esser and D. Hennig, *Philos. Mag. B* **65**, 887 (1992).
- [13] D. Hennig, *Phys. Scr.* **46**, 14 (1992).
- [14] D. Hennig, *J. Phys. A* **25**, 285 (1992).
- [15] D. Hennig and B. Esser, *Phys. Rev. A* **46**, 4569 (1992).
- [16] V. M. Kenkre and G. P. Tsironis, *Phys. Rev. B* **35**, 1473 (1987).
- [17] V. M. Kenkre and H.-L. Wu, *Phys. Lett. A* **135**, 120 (1989).
- [18] V. M. Kenkre and H.-L. Wu, *Phys. Rev. B* **39**, 6907 (1989).
- [19] P. Grigolini, H.-L. Wu, and V. M. Kenkre, *Phys. Rev. B* **40**, 7045 (1989).
- [20] G. P. Tsironis and V. M. Kenkre, *Phys. Lett. A* **127**, 209 (1989).
- [21] G. P. Tsironis, V. M. Kenkre, and D. Finley, *Phys. Rev. A* **37**, 4474 (1988).
- [22] M. I. Salkola, A. R. Bishop, V. M. Kenkre, and S. Raghavan, *Phys. Rev. B* **52**, R3824 (1995).
- [23] H. Schanz and B. Esser, *Z. Phys. B* **101**, 1299 (1996).
- [24] H. Schanz and B. Esser, *Phys. Rev. A* **55**, 3375 (1997).
- [25] R. Graham and M. Höhnerbach, *Phys. Lett.* **101A**, 61 (1984).
- [26] R. Steib, Diplomarbeit, Universität Ulm, 1995.
- [27] M. A. M. de Aguiar, K. Furaya, C. H. Lewenkopf, and M. C. Nemes, *Ann. Phys. (N.Y.)* **216**, 219 (1992).
- [28] C. H. Lewenkopf *et al.*, *Phys. Lett. A* **155**, 113 (1991).
- [29] L. Müller, J. Stolze, H. Leschke, and P. Nagel, *Phys. Rev. A* **44**, 1022 (1991).
- [30] E. T. Jaynes and F. W. Cummings, *Proc. IEEE* **51**, 89 (1963).
- [31] M. Tavis and F. W. Cummings, *Phys. Rev.* **170**, 379 (1968).
- [32] M. Tavis and F. W. Cummings, *Phys. Rev.* **188**, 692 (1969).
- [33] H. A. Jahn and E. Teller, *Proc. R. Soc. London, Ser. A* **161**, 220 (1937).
- [34] P. Kramer and M. Saraceno, *Geometry of the Time-Dependent Variational Principle in Quantum Mechanics*, edited by J. Ehlers, K. Hepp, R. Kippenhahn, H. A. Weidenmüller, and J. Zittartz, *Lecture Notes in Physics* Vol. 140 (Springer-Verlag, Berlin, 1981).
- [35] B. Esser and H. Schanz, *Z. Phys. B* **96**, 553 (1995).
- [36] W. H. Press, B. P. Flannery, S. A. Teukolsky, and W. T. Vetterling, *Numerical Recipes in C* (Cambridge University Press, Cambridge, England, 1988).
- [37] M. Hénon, *Physica D* **5**, 412 (1982).
- [38] R. Graham and M. Höhnerbach, *Z. Phys. B* **57**, 233 (1984).
- [39] K. E. Cahill and R. J. Glauber, *Phys. Rev.* **177**, 1857 (1969).
- [40] W. Magnus, F. Oberhettinger, and R. P. Soni, *Formulas and Theorems for the Special Functions of Mathematical Physics* (Springer-Verlag, Berlin, 1966).
- [41] M. Cibils, Y. Cuche, and G. Müller, *Z. Phys. B* **97**, 565 (1995).
- [42] R. J. Glauber, *Phys. Rev.* **131**, 2766 (1963).
- [43] W.-M. Zhang, D. H. Feng, and R. Gilmore, *Rev. Mod. Phys.* **62**, 867 (1990).
- [44] A. Perelomov, *Generalized Coherent States and Their Applications* (Springer-Verlag, Berlin, 1986).
- [45] J. K. Klauder and B. Skagerstamm, *Coherent States, Applications in Physics and Mathematical Physics* (World Scientific, Singapore, 1985).
- [46] P. A. M. Dirac, *Proc. Cambridge Philos. Soc.* **26**, 376 (1930).